

Dihadron correlations in PbPb collisions at $\sqrt{s_{NN}} = 2.76$ TeV with CMS

Jeremy Callner for the CMS Collaboration

University of Illinois at Chicago, Chicago, IL, USA

E-mail: jcallner@gmail.com

Abstract. Measurements of charged dihadron $\Delta\eta$ – $\Delta\phi$ correlations from the CMS collaboration are presented for PbPb collisions at a center-of-mass energy of 2.76 TeV per nucleon pair over a broad range of pseudorapidity and the full range of azimuthal angle. A significant correlated yield is observed for pairs of particles with small $\Delta\phi$ but large longitudinal separation $\Delta\eta$, commonly known as the “ridge”. The ridge persists up to at least $|\Delta\eta| = 4$ and the dependence of the ridge region shape and yield on collision centrality and transverse momentum has been measured. A Fourier analysis of the long-range two-particle correlation is presented and discussed in the context of higher order flow coefficients.

The starting point of this dihadron correlations analysis is the two-dimensional (2-D) per-trigger-particle associated yield as a function of $\Delta\eta$ and $\Delta\phi$ for all particles falling within a given “trigger” (p_T^{trig}) and “associated” (p_T^{assoc}) transverse momentum interval. The CMS silicon tracker [1], with its large pseudorapidity coverage, is ideally suited for detailed analyses of both short- and long- range charged hadron correlations at the LHC. Dihadron correlation results from CMS in the 0–5% most central PbPb collisions have recently been reported in Ref. [2], which found several non-trivial features including a significant broadening of the away side ($\Delta\phi > 1$) dihadron correlation when compared to pp collisions and a prominent near side ridge centered at $\Delta\phi \approx 0$ with an associated yield that decreases as a function of increasing transverse momentum above 6 GeV/ c . The current analysis extends the results to 12 centrality classes and also explores in detail the resulting structure and its possible connection with collective motion as manifest in a Fourier analysis of the $\Delta\phi$ associated yield distribution.

An example of the resulting 2-D correlations for trigger particles with $4 < p_T^{\text{trig}} < 6$ GeV/ c and associated particles with $2 < p_T^{\text{assoc}} < 4$ GeV/ c is shown in Fig. 1 for two selected centrality classes. The 2-D associated yield distributions reveal a rich structure and evolution as a function of centrality. Of most relevance to the current investigation is the ridge yield centered at $\Delta\phi \approx 0$ and extending to $|\Delta\eta| = 4$. In mid-peripheral collisions, a pronounced $\cos(2\Delta\phi)$ component emerges, presumably originating from the elliptic flow effect and similar in character to what has been observed at RHIC energies [3, 4, 5].

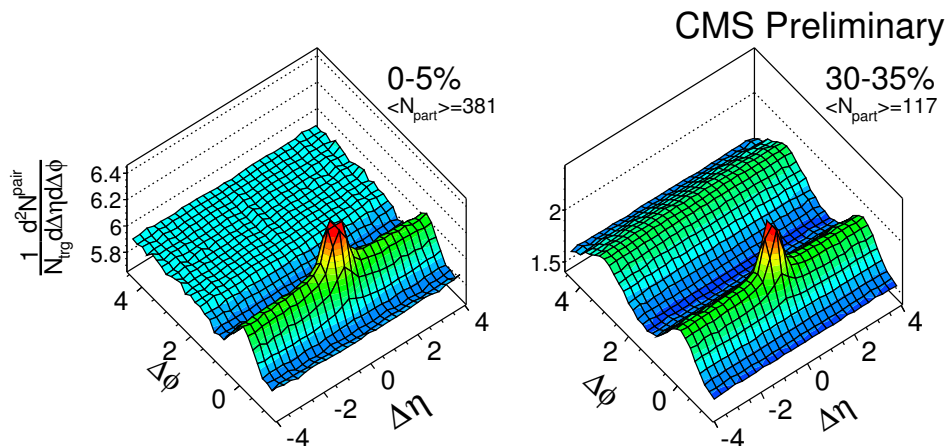


Figure 1. Two-dimensional (2-D) per-trigger-particle associated yield of charged hadrons as a function of $\Delta\eta$ and $\Delta\phi$ for $4 < p_T^{\text{trig}} < 6$ GeV/c and $2 < p_T^{\text{assoc}} < 4$ GeV/c in central (left) and mid-peripheral (right) PbPb collisions at $\sqrt{s_{NN}} = 2.76$ TeV.

To quantitatively examine the features of short- and long- range azimuthal correlations, one dimensional (1-D) $\Delta\phi$ correlation functions are calculated by averaging the 2-D distributions over a selected region in $\Delta\eta$. The zero-yield-at-minimum (ZYAM) methodology applied to the resulting 1-D $\Delta\phi$ correlation enables the extraction of the integrated associated yields in the near-side jet and ridge regions around $\Delta\phi \approx 0$, as outlined in Ref. [2]. The ZYAM methodology is also applied in this analysis for the $\Delta\phi$ distributions, with the results shown in Fig. 2(a). Two distinct regions in $|\Delta\eta|$ are studied independently; the short-range “Jet Region” centered at $(\Delta\eta, \Delta\phi) \approx (0, 0)$ and the long-range “Ridge Region” at larger $|\Delta\eta|$ from 2 to 4 units. A strong centrality dependence is observed in the associated yields that comes primarily from the long-range ridge region. By subtracting off the ridge region yield from the jet region yield, the residual jet region associated yield is found to be largely independent of centrality, a general feature of the data that is similar to that seen at RHIC [6, 7].

The pronounced $\cos(2\Delta\phi)$ component visible in the 2-D correlations has been associated with the elliptic flow v_2 collective motion, and thus it is desirable to subtract this component from the dihadron correlations in order to study the residual yield [8]. This analysis was performed utilizing the CMS results for elliptic flow [9] with additional details on the subtraction methodology given in Ref. [10]. The elliptic flow v_2 subtracted associated yield for the ridge region is given in Fig. 2(b). The most prominent feature of the v_2 -subtracted result is that the remaining ridge region yield is found to be negligible for lower N_{part} values, and increases roughly linearly to an N_{part} value of around 300. This general feature of the v_2 -subtracted ridge yield is similar to that seen at lower energies [11], where the associated yield was found to drop to zero below $N_{part} \approx 100$. This analysis indicates that many of the centrality dependent features of the ridge yield in PbPb collisions at $\sqrt{s_{NN}} = 2.76$ TeV, for our selected trigger and associated momentum ranges, are very similar in character to what has been observed in lower energy AuAu collisions at $\sqrt{s_{NN}} = 0.2$ TeV.

Motivated by the idea of understanding the long-range ridge effect in the context

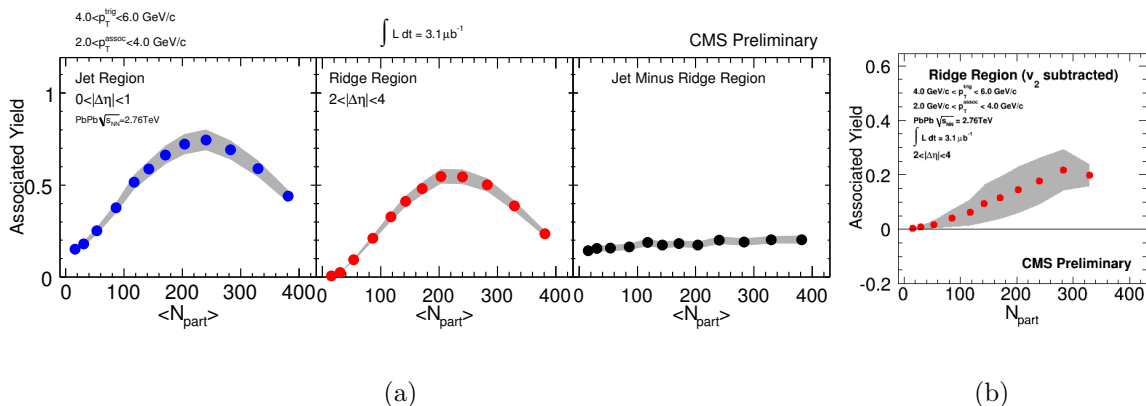


Figure 2. (a) Integrated near-side associated yields for $4 < p_T^{\text{trig}} < 6$ GeV/ c and $2 < p_T^{\text{assoc}} < 4$ GeV/ c , above the minimum level found by the ZYAM procedure, for (left) the jet region ($0 < |\Delta\eta| < 1$), (middle) the ridge region ($2 < |\Delta\eta| < 4$), and difference of jet-ridge region (right) as a function of N_{part} for PbPb collisions at $\sqrt{s_{NN}} = 2.76$ TeV. (b) Integrated near-side associated yield for the ridge region with the CMS measured elliptic flow v_2 component subtracted. The gray bands correspond to systematic uncertainties [10].

of higher-order hydrodynamic flow (e.g. induced by initial geometric fluctuations [12]) an alternative way of quantifying the observed long-range correlations using a Fourier decomposition technique is investigated. Following the methodology of [2], the $\Delta\phi$ distribution is decomposed into a Fourier series using the following expression:

$$\frac{1}{N_{\text{trig}}} \frac{dN^{\text{pair}}}{d\Delta\phi} = \frac{N_{\text{assoc}}}{2\pi} \left(1 + \sum_{n=1}^{\infty} 2C_n^f \cos(n\Delta\phi) \right), \quad (1)$$

where N_{assoc} represents the total number of dihadron pairs per trigger particle for a given $|\Delta\eta|$ range and $(p_T^{\text{trig}}, p_T^{\text{assoc}})$ bin. The result of the Fourier analysis is that the observed 1-D $\Delta\phi$ projections in the ridge region are well described by the first five terms in the series. If the observed correlation is purely driven by the single-particle azimuthal anisotropy arising from the hydrodynamic expansion of the medium [13], the extracted Fourier C_n^f components would be related to the flow coefficients v_n via:

$$C_n^f(p_T^{\text{trig}}, p_T^{\text{assoc}}) = v_n^f(p_T^{\text{trig}}) \times v_n^f(p_T^{\text{assoc}}), \quad (2)$$

where $v_n^f(p_T^{\text{trig}})$ and $v_n^f(p_T^{\text{assoc}})$ can be identified with the flow coefficients for the trigger and associated particles as extracted from this type of Fourier analysis. Non-flow effects on the extracted v_n^f values can be minimized by fixing the associated particles at low p_T values where hydrodynamic flow should dominate. Following the assumption in Eq. 2, the hydrodynamic flow v_n^f harmonics as a function of p_T^{trig} can be extracted from the measured C_n^f values as follows:

$$v_n^f(p_T^{\text{trig}}) = \frac{C_n^f(p_T^{\text{trig}}, p_T^{\text{assoc}})}{v_n^f(p_T^{\text{assoc}})}, \quad (3)$$

where $v_n^f(p_T^{\text{assoc}})$ can be calculated as $\sqrt{C_n^f(p_T^{\text{trig}}, p_T^{\text{assoc}})}$ for both p_T^{trig} and p_T^{assoc} in the same range as the one chosen for p_T^{assoc} , which for this analysis was selected as

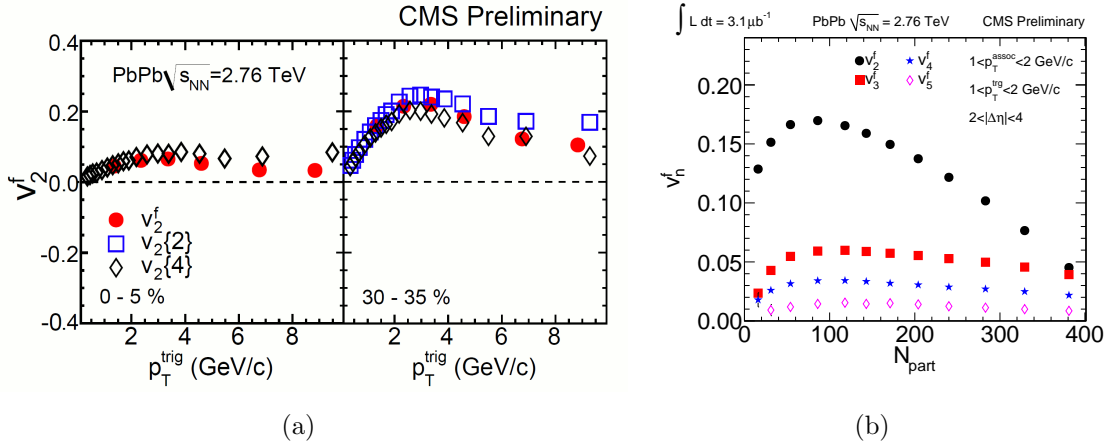


Figure 3. (a) v_2^f hydrodynamic harmonic extracted as a function of p_T^{trig} for $1 < p_T^{\text{assoc}} < 2$ GeV/c for central (left) and mid-peripheral (right) PbPb collisions at $\sqrt{s_{NN}} = 2.76$ TeV. Comparisons to the two- and four-particle cumulant method of measuring v_2 (b) The flow harmonics v_2^f , v_3^f , v_4^f and v_5^f extracted from long-range ($2 < |\Delta\eta| < 4$) azimuthal dihadron correlations for $1 < p_T^{\text{trig}} < 2$ GeV/c and $1 < p_T^{\text{assoc}} < 2$ GeV/c as a function of the number of participating nucleons (N_{part}) in PbPb collisions at $\sqrt{s_{NN}} = 2.76$ TeV. [9] are also shown. Statistical and systematic uncertainties are negligible.

$1 < p_T^{\text{assoc}} < 2$ GeV/c. The extracted v_2^f are shown in Fig. 3(a) as a function of p_T^{trig} for central and mid-peripheral collisions. The results are found to be in good agreement with elliptic flow values measured by standard flow methods [9]. Fig. 3(b) gives the centrality dependence of the extracted flow coefficients at low p_T for the higher harmonics $n=2$ to 5. The strong centrality dependence of v_2^f matches expectation from standard elliptic flow analyses, and the observed much weaker centrality dependence of the higher harmonics, as well as their observed relative strengths, awaits a more quantitative comparison to other data and theory.

References

- [1] R. Adolphi *et al.* [CMS Collaboration], JINST **3**, S08004 (2008).
- [2] CMS Collaboration, arXiv:1105.2438.
- [3] STAR Collaboration, Phys. Rev. Lett. **95** (2005) 152301.
- [4] PHENIX Collaboration, Phys. Rev. Lett. **98** (2007) 232302.
- [5] PHOBOS Collaboration, Phys. Rev. **C81** (2010) 024904.
- [6] STAR Collaboration, J. Phys. G: Nucl. Part. Phys. **34** (2007) S679.
- [7] STAR Collaboration, Phys. Lett. **B683** (2010) 123.
- [8] STAR Collaboration, Phys. Rev. **C80** (2009) 064912.
- [9] CMS Collaboration, CMS Physics Analysis Summary, **HIN-10-002** (2011).
- [10] CMS Collaboration, CMS Physics Analysis Summary, **HIN-11-006** (2011).
- [11] PHOBOS Collaboration, Phys. Rev. Lett. **104** (2010) 062301.
- [12] B. Alver and G. Roland, Phys. Rev. **C81** (2010) 054905.
- [13] S. Voloshin and Y. Zhang, Z. Phys. **C70** (1996) 665.